Title

Selective Molecular Recognition and Indicator Displacement Sensing of Neurotransmitters in Cellular Environments

Journal

ACS Sensors, 8(8)

ISSN

2379-3694

Authors

Chen, Junyi

Tabaie, Emily Z

Hickey, Briana L

et al.

Publication Date

2023-08-25

DOI

10.1021/acssensors.3c00886

Selective Molecular Recognition and Indicator Displacement Sensing of Neurotransmitters in Cellular Environments

Junyi Chen,[2] Emily Z. Tabaie,[3] Briana L. Hickey,[1] Ziting Gao,[1] Alexie Andrea P. Raz,[1] Zongbo Li,[1] Emma H. Wilson,[3] Richard J. Hooley[1,2,3]* and Wenwan Zhong[1,2,3]*

* E-mail: richard.hooley@ucr.edu; wenwan.zhong@ucr.edu

[1]Department of Chemistry; [2]Environmental Toxicology Graduate Program; [3]Division of Biomedical Sciences; University of California – Riverside, Riverside, CA 92521, U.S.A.

ABSTRACT: Flexible, water-soluble hosts are capable of selective molecular recognition in cellular environments, and can detect neurotransmitters such as choline in cells. Both cationic and anionic water-soluble self-folded deep cavitands can recognize suitable styrylpyridinium dyes in cellular interiors. The dyes selectively accumulate in nucleotide-rich regions of the cell nucleus and cytoplasm. The hosts bind the dyes and promote their relocation to the outer cell membrane: the lipophilic cavitands predominantly reside in membrane environments, but are still capable of binding suitable targets in other cellular organelles. Incubating the cells with structurally similar biomarkers such as choline, cholamine, betaine or butyrylcholine illustrates the selective recognition. Choline and butyrylcholine can be bound by the hosts, but minimal binding is seen with betaine or cholamine. Varying the dye allows control of the optical detection method, and both "turn-on" and "turn-off" sensing is possible.

KEYWORDS: *sensors, molecular recognition, intracellular sensing, host:guest complexes, fluorescence imaging, indicator displacement.*

Macrocyclic synthetic receptors are a powerful tool for the recognition and sensing of biorelevant molecules.[1] This, of course, requires the receptors to be functional in biomedia. There are many water-soluble macrocyclic hosts in the literature, from cyclodextrins, calixarenes, cucurbit[n]urils, cyclophanes, pillararenes and self-folding cavitands.[2] While there are myriad examples of these hosts being used for selective recognition in buffered solution, more complex environments such as urine, saliva, serum, lipid membranes and living cells provide a much greater challenge.[3] Even high salt concentrations can be a problem:[4] for example, CB[7] is one of the most effective macrocyclic hosts known, but its target affinity is weakened by high concentrations of sodium salts.[5] Each type of receptor has its strengths and weaknesses, and effective recognition in aqueous solution does not necessarily translate to complex biomedia. Despite these challenges, the application of macrocyclic receptors *in vitro* is an enticing target for biosensing, drug delivery and therapeutic development.[6] As well as *recognition* of biological targets in cells, effective sensing requires a reporting element: in the case of macrocyclic receptors, this is most often an indicator displacement assay.[7] This introduces further challenges for function in cells: not only must the host selectively bind the target in the presence of all the interferents in a cell, it must also bind the indicator and give a strong signal response upon displacement: this limits the scope of suitable receptors.

The super-high affinity of cucurbiturils for diamines allows their function in cells, and they have been used to monitor intracellular redox processes,[8] bind proteins,[9] and can be used in drug delivery or remediation[10] and imaging.[11] The most successful examples of macrocyclic hosts being used in cells for molecular recognition and sensing are Guo's micellar calixarene aggregates, which allow drug delivery, phototheranostics and bioimaging.[12] Creating supramolecular nanoparticles alleviates some of the drawbacks of individual receptors, but is not applicable to host types that are more difficult to derivatize. The use of individual, non-aggregated receptors in cells is far rarer, as their lower selectivity and target affinity restrict their use. Nau showed indicator displacement assays with tetrasulfonato-calixarene and lucigenin dye in live cells that were able to detect species such as choline, acetylcholine or protamine.[13] Neri used calixarenes for affinity pull-down in cancer cells[14] and Guo used non-aggregated azacalixarenes to monitor hypoxia via Indicator Displacement Assay (IDA),[15] but there is still a dearth of applications of macrocyclic molecular recognition in cells, or studies about the localization of those hosts on cell interiors.

Water-soluble, self-folding deep cavitands have many advantages over more rigid macrocycles in selective molecular recognition of biorelevant targets:[16] they can be easily functionalized with different motifs at the upper and lower rim, and the large cavities can bind many different fluorescent dyes.[17] They can display multiple orthogonal recognition mechanisms, which allows the selective sensing of targets as diverse as post-translationally modified peptides,[17a,b] kinase substrates,[17c] various DNA secondary structures,[17d-f] drugs of abuse[17g] and insect pheromones.[17h] While they are functional in complex biomedia, such as urine, saliva and serum, we have only rarely been successful when applying them in living cells. The lipophilic cavitand **TCC**[18] was able to bind a trimethylammonium ($R\text{-}NMe_3^+$) - tagged fluorescein derivative and accelerate its delivery into HeLa cells and via cavitand-mediated endocytosis.[19] The weakness with that system was that the dye was released from the cavitand once on the cellular interior, and trapped in endosomes, not suitable for IDA nor for study of host-guest interaction in cellular environments. This, however, was a facet of the *dye*, not the cavitand: in the intervening period, we have synthesized a far wider range of suitable dyes

for this host.[17] Here, we show that water-soluble hosts can perform selective molecular recognition and indicator displacement assays inside living cells, and alter the intracellular location of fluorophores *via* selective molecular recognition.

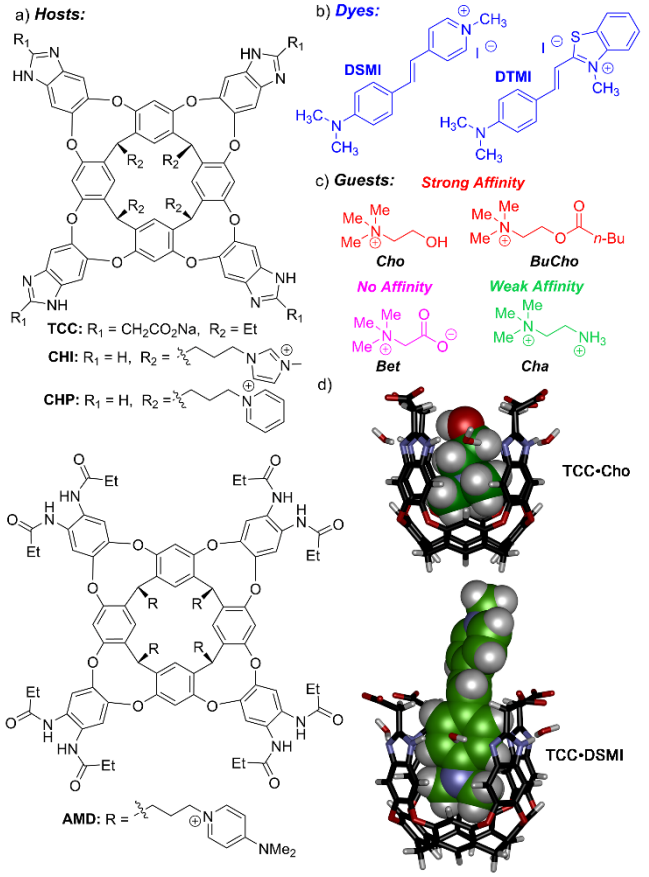

Figure 1. The structures of a) hosts, b) guests and c) indicator dyes used in this study. d) minimized structures of the **TCC•Cho** and **TCC•DSMI** host:guest complexes (SPARTAN, semi-empirical, lower rim ethyl groups omitted for clarity).

RESULTS AND DISCUSSION

The cavitands, dyes and guests tested are shown in Figure 1. Styrylpyridinium dyes **DSMI** and **DTMI** show strong (K_d ~5-50 μM) affinity for multiple different deep cavitands in buffer,[17d,f,g] binding with the aniline group inside the host cavity, and display enhanced fluorescence when bound. The dyes each bind DNA,[17d-f] and would be expected to localize into cellular compartments that contain nucleic acids: for example, it has been shown that a similarly structured dye, the -NH_2 equivalent of **DSMI** locates at the nucleoli and mitochondria[20] upon addition to cells. To establish their intracellular behavior, the two dyes (**DSMI** and **DTMI**) were incubated in HeLa cells in PBS solution (5 μM dye) for 1 h. Both dyes were transported into the cell and could be observed upon confocal microscopy. Interestingly, washing the cells with a PBS buffer solution (as a control to mimic the subsequent addition of other species) caused the **DSMI** dye to be washed out of the cell interiors, whereas **DTMI** was retained, and showed a significantly higher fluorescence emission with the same concentration and incubation time. Each of the dyes showed a preference for clustering in specific locations in the cell, notably nucleotide-rich areas (Figures S-1 – S-4): while **DTMI** stained the complete nucleus, **DSMI** clustered in the nucleolus, and both dyes in the cytoplasm had a colocalization coefficient > 0.67 with that of MitoView650 (Figures 2 and S-2 and S-4), indicating the staining of mitochondria. We have previously shown that both **DSMI** and **DTMI** have strong affinity for folded nucleic acid strands (and concomitant fluorescence enhancement) in buffered solution:[17d,f] the affinity for nucleotide-rich regions of the cell is consistent with that observation. The specific location of **DSMI** in the nucleolus, which contains the ribosomal machinery, rather than the entire nucleus, may be worthy of future investigation.

Next, the effects of cavitand host were tested. Four different types of cavitand were used: anionic **TCC** and cationic **CHI**/**CHP** show a kinetically stable folded "vase" conformation in water and bind styrylpyridinium dyes strongly,[17] whereas cationic octamide cavitand **AMD** is more flexible.[17f] Unfortunately, **CHI** and **CHP** cavitands were unsuitable for cell transport as they formed large insoluble aggregates with both dyes (Figure S-25). Despite their structural similarities to the unsuccessful hosts, the **TCC** and **AMD** hosts were far more interesting. The initial questions were whether the different hosts could bind the dyes in cellular environments, and what effect that binding had on their location and fluorescence emission. The more well-known host **TCC** was tested first. Two addition strategies were used: either the dye was added to the cells and incubated for 1 h, followed by addition of cavitand (termed "**seq-mix**" for clarity), or the host and dye were premixed (forming a **host•dye** complex, termed "**pre-mix**"), and that solution was added to the cells. The difference between these addition methods was not easily predictable, as the host•dye complexation is rapid and reversible (in/out exchange with **TCC** occurs on the order of ~10/s at ambient temperature in water[18b]). While the affinity for the dyes in **TCC** is on the order of micromolar, the binding is non-covalent, and this rapid exchange allows equilibration between the bound and free states. As such, bound dye could theoretically be sequestered by the cavitand in the cell, or released into the cytosol, and both outcomes are possible with each addition strategy.

Five μM **DSMI** dye was premixed with 5 μM **TCC** in PBS buffer and added to the HeLa cells, followed by a PBS wash and 1 h incubation ("pre-mix"). Interestingly, adding the pre-mixed **TCC•DSMI** does not suffer any loss of **DSMI** stain from the cell interior after washing with PBS: despite an identical washing procedure, no loss of **DSMI** is seen in the presence of cavitand, whereas all dye could be removed from the cells in its absence (see Figures S-2). These results suggest a persistent **TCC•DSMI** host:guest complex in the cell. In addition, the intracellular location of the dye is substantially altered (Figure 2). Whereas the free dye localized in nucleotide-rich areas, in the presence of an equimolar concentration of cavitand **TCC**, the observed fluorescence is almost completely localized in the external plasma membrane, and the colocalization coefficient with that of MitoView650 reduced to 0.41. The effectiveness of this recognition is quite remarkable: while the ability of **TCC** to form strong complexes with dyes such as **DSMI** is known (K_d = 5.2 μM in buffer),[17c] **DSMI** also has micromolar affinity for short strands of DNA.[17d-f] Despite the large nucleotide concentration in the cell, the cavitand is able to retain the dye in its cavity, and sequester the **TCC•DSMI** complex in the membrane. The lipophilic **TCC** is well-known to bind in synthetic lipid bilayers such as POPC vesicles, micelles or supported lipid bilayers,[21] but this is the first evidence that supports that in a living cell. The same behavior can be seen with the

DTMI, but it requires more **TCC** cavitand than needed by **DSMI**. While a 1:1 ratio (5 μM each, pre-mix) of **TCC** and **DSMI** causes the dye to be sequestered in the membrane, the same result is only seen with a 4:1 ratio of **TCC:DTMI** (20:5 μM, Figures S-7 – S-10). As the affinity of **DTMI** for **TCC** (K_d = 8.9 μM in buffer[17f]) is quite similar to that of **DSMI**, this result suggests that the **DTMI** dye has a greater affinity for other cellular constituents.

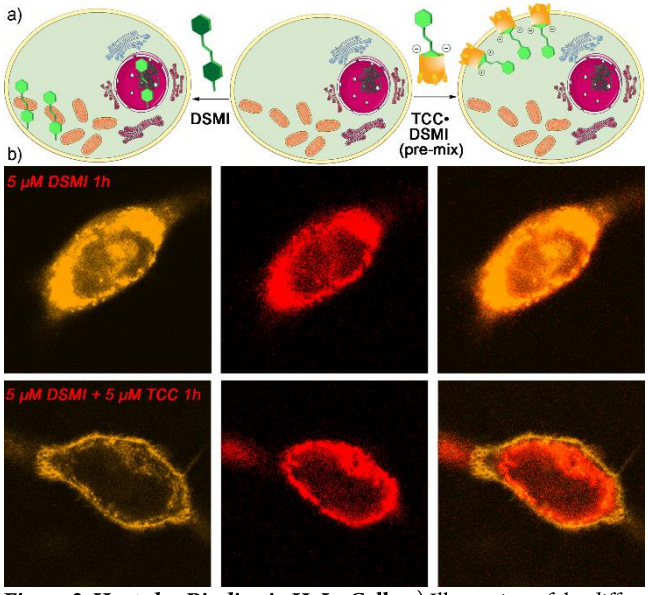

Figure 2. Host:dye Binding in HeLa Cells. a) Illustration of the different cellular locations shown by **DSMI** and the **TCC•DSMI** premixed complex. b) Confocal fluorescence images of live HeLa cells treated by 5 μM **DSMI** for 1 h (top), and 5 μM **DSMI•TCC** (**pre-mix**) for 1 h (bottom). The images of 2 channels including both **DSMI**, and MitoView650, as well as their Merged images, are listed from left to right. See Figure S-1 for full size images of all channels.

To shed more light on these differences, the incubation was repeated sequentially, i.e. 5 μM dye was incubated with the HeLa cells for 1 h, followed by addition of cavitand. **DSMI** is not ideal for this purpose, as the addition of buffer washes the dye from the cells. When 5 μM **TCC** was added to cells containing 5 μM **DSMI** (**seq-mix**), not all of the dye was lost, but the low concentration complicated the confocal microscopy experiments. As such, we focused on the effects of **TCC** cavitand on cell-bound **DTMI** (Figure 3). To most clearly show the location of the **DTMI•TCC** complex, the images in Figure 3 were taken with a Gain that allows visualization of the darker **DTMI•TCC** in the membrane, so the cells with unbound **DTMI** are very bright. Please see Figure S-4 for lower Gain images that more clearly show the location of **DTMI** in the absence of **TCC**.

The cells were incubated with 5 μM **DTMI** for 1 h, followed by addition of 20 μM **TCC**. We selected 100 cells from the total of 10 images taken at various locations, and monitored the change in each cell's fluorescence intensity over time by confocal microscopy (a subset of 10 cells is shown in Figure 3a-e, for others, see Figures S-13 – S-16). Over time, the strong emission shown by **DTMI** when bound in nucleotide-rich regions of the cell dissipates, and the fluorescence is slowly moved to the outer membrane. The rate of fluorescence change is not consistent between different cells, as would be expected, but in some of the cells, the dye was displaced from the nucleotide-rich region in < 15 mins, and moved to the plasma membrane. These results indicate that the **TCC** host can be rapidly incorporated into the cells and binds to the dye. We had previously shown that **TCC** is endocytosed by cells,[19] and this experiment shows that the cavitand is not sequestered in endosomes, but can easily move into the cytoplasm to compete with the nucleotides for dye binding. Most importantly, while the fluorescence of the **TCC•dye** complexes is observed in the outer membrane, the cavitand is not permanently sequestered there. The images in Figure 3 clearly show that the **TCC** host can access **DTMI** dye bound in the mitochondria/nucleolus, outcompete the nucleotides in those regions for the **DTMI** dye, and relocate the **TCC•DTMI** complex to the outer membrane in less than 2 h. The Violin plot of the mean integrated fluorescence intensity changes measured on 100 cells also clearly showed two cell populations, one with higher fluorescence intensity from **DTMI** residing at the nucleotide-rich regions, and the other with lower intensity with **DTMI** translocated to the membrane by **TCC**. The lower intensity population appeared 15 mins after the addition of **TCC**, and continued to increase with longer incubation duration. When simple PBS buffer incubation was used as control, we did not observe any location change of the dye, nor any differentiation of high- and low-intensity cell populations. Instead, the fluorescence of each cell dropped continuously due to simple washing of the dye from the cells over time (Figures S-17 – S-18). It should be noted that the amounts of cavitand used are small in each case – an equimolar amount of **TCC** can relocate **DSMI** in the cell, and only four equivalents are needed for **DTMI**. The recognition is strong and efficient in the complex environment of the cell. Both dyes exhibit a lower fluorescence emission *via* microscopy in the presence of **TCC** than free in the cells. This is because dye incorporation in nucleotides increases the emission of the two dyes far more than binding in the host,[17c,f] so a "turn-off" effect is observed upon cellular formation of the **TCC•dye** complexes in each case. Free **DTMI** in cells is brighter than **DSMI**, because **DTMI** is brighter when DNA-bound: we have previously shown that **DTMI** exhibits higher fluorescence than **DSMI** when bound to DNA G-quadruplexes.[17f]

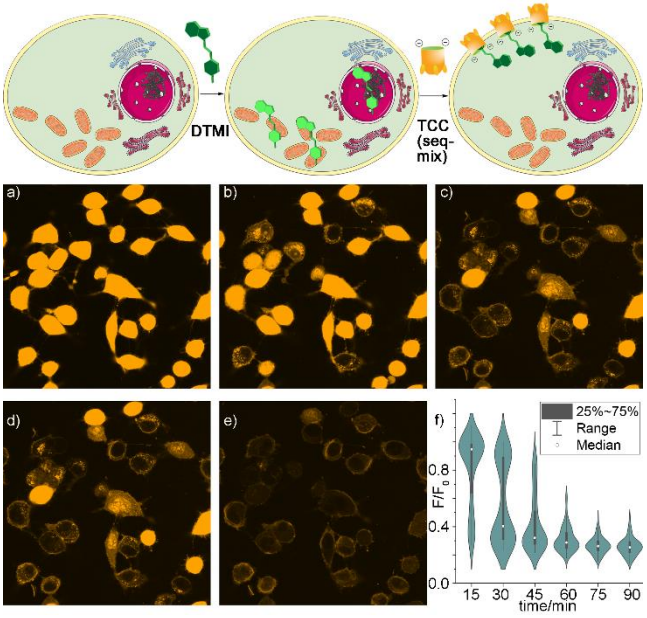

Figure 3. Intracellular Relocation. Confocal fluorescence images of live HeLa cells treated by 5 μM **DTMI** for 1 h, followed by incubation with 20 μM **TCC** (seq-mix) for a-e) 0, 15, 30, 45, and 75 mins. f) Violin plot of the integrated density (F) change over time measured on each

individual cell (n = 100). F_0, the fluorescence measured at t = 0 min. All images taken with identical Gain, to show the location of the **TCC•DTMI** complex – for lower Gain images that show the **DTMI** location more clearly, see Figure S-4.

These studies illustrate the ability of the host to perform selective molecular recognition and translocation of styrylpyridinium dyes in HeLa cells. The more interesting question, however, is whether this recognition can be outcompeted by an added guest, enabling a selective indicator displacement assay. To test this, a set of biologically important substrates for the cavitands were tested, some of which had been tested by Nau in his paper.[13] These substrates are shown in Figure 1, and consist of variably functionalized trimethylammonium ($R\text{-}NMe_3^+$) ions. Choline (**Cho**), butyrylcholine (**BuCho**) and cholamine (**Cha**) are signaling molecules, involved in neurological function or immune response, and betaine (**Bet**) is a choline metabolite that can be a predictor of adverse cardiovascular events.[3f] While superficially similar in structure, these substrates show highly variable affinity for **TCC** in aqueous solution: **Cho** and **BuCho** bind strongly (K_d ~ 10 μM), with the NMe_3^+ group in the cavity of the host.[18a] **Bet** shows no affinity, as the anionic carboxylate provides Coulombic repulsion with the upper rim carboxylates in **TCC** upon binding. **Cha** shows variable affinity, depending on the conditions: it effects precipitation of the host in pure water,[18a] but can be bound at low cavitand concentrations[17b] or in lipid environments.[21]

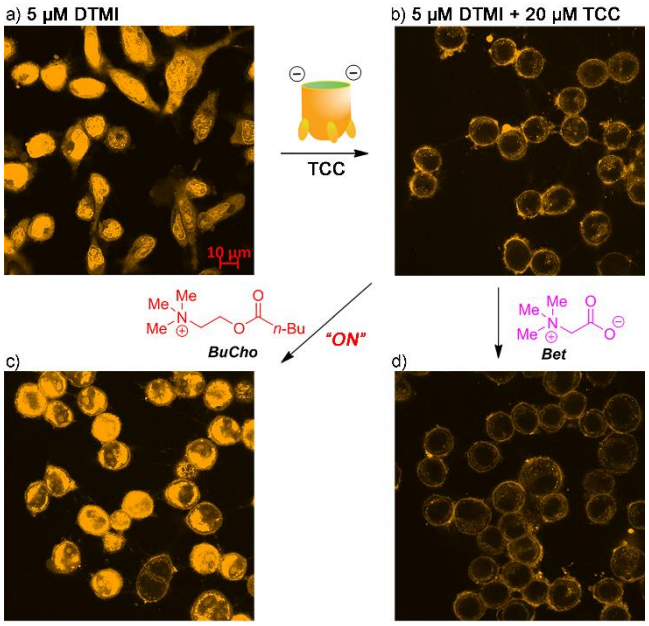

Figure 4. IDA sensing with TCC•DTMI. DTMI channel fluorescence images of live HeLa cells treated by a) 5 μM **DTMI**, b) **TCC•DTMI** (pre-mix, 20 μM, 5 μM); c) **TCC•DTMI** (pre-mix, 20 μM, 5 μM) + 50 mM Butyrylcholine; d) **TCC•DTMI** (pre-mix, 20 μM, 5 μM) + 50 mM Betaine. Incubation time = 1 h. Image a) was captured under a lower Gain = 700.0, images b), c), d) were captured under Gain = 800.0 and larger pinhole.

Each of these guests (50 mM concentration) were added to HeLa cells containing **TCC** and either of the two dyes. The cell permeability of small organic ions such as choline is quite low,[13] hence the need for a high added concentration of analyte - the concentration in the cells is much smaller. Figure 4 shows the effect of adding butyrylcholine or betaine to the cell-bound **TCC•DTMI** (for full images of the additions of other substrates including **Cho** and **Cha**, see Figures S-11 and S-12). The images show that the **TCC** host is capable of selective indicator displacement assays with variable $R\text{-}NMe_3^+$ ion substrates in living cells. The strongly bound guests (**Cho**, **BuCho**) cause displacement of each dye from the **TCC** host after 1 h incubation. This indicates that the added guests are transported into the cells and can outcompete the dye for binding in membrane-bound **TCC**. In contrast, the weakly bound guest **Bet** has no effect on the emission: despite the small change in structure, this guest does not bind in the host, as the anionic carboxylate provides a deleterious interaction with the electron-rich cavitand walls. **Cha** is more ambiguous: displacement occurs, but to a much lower extent than with **Cho**, suggesting that the host can bind **Cha** in the cellular environment, but the affinity is much lower. The **TCC•DTMI** system is a selective, "turn-on" sensor for strongly binding guests (**Cho**, **BuCho**) due to indicator displacement, followed by a relocation of the dye to its "free" locations (nucleotide-rich regions of the mitochondria and nucleus), rather than the outer membrane. Weakly bound guests (**Bet**) cause no displacement and no change in emission. **DTMI** has a very strong increase in emission when released from the host and bound in nucleotide-rich cellular regions. When **Cho** is bound in the cavitand, the emission increase is so large that the images must be captured under lower gain value to visualize the dye properly (see Figures S-11 and S-12). Addition of **BuCho** causes a slightly lower increase in dye emission, so the images in Figure 4 were all obtained with the same gain.

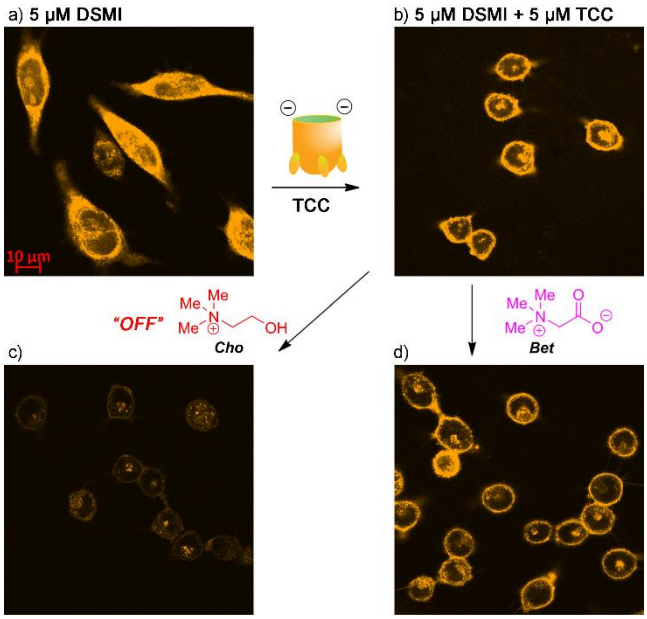

Figure 5. IDA sensing with TCC•DSMI. DSMI channel fluorescence images of live HeLa cells treated by a) 5 μM **DSMI** for 1 h; b) **TCC•DSMI** (pre-mix, 5 μM each) then PBS for 1 h; c) **TCC•DSMI** (pre-mix, 5 μM each) then 50 mM Choline for 1 h; d) **TCC•DSMI** (pre-mix, 5 μM each) then 50 mM Betaine for 1 h.

While the two dyes illustrate the indicator displacement assay efficiently, the visual results are quite different. Whereas the **TCC•DTMI** pair is a "turn-on" sensor, **DSMI** is washed from the cell after displacement, and thus can act as a "turn-off" sensor. For example, in Figure 5, the **TCC•DSMI** complex is located in the outer membrane. After addition of the weakly bound **Bet**, no displacement occurs, and no change is seen. Addition of **Cho** washes

the dye from both the **TCC** host and the cell, so the observed fluorescence is significantly *reduced*. While the target recognition properties of the **TCC** host remain unchanged, changing the dye allows different fluorescent readouts of the binding event.

The confocal microscopy images are useful for a qualitative determination of the IDA process, and illustrate the location of the dye, but flow cytometry provides a more quantitative analysis of dye fluorescence change during host recognition and guest displacement (Figure 6). The flow cytometry experiments nicely illustrate the "turn-off" and "turn-on" mechanisms for the two dyes (**DSMI** and **DTMI** respectively). The fluorescence center for **DSMI** was minimally shifted when incubated with **TCC** for 1h (Figure 6c, red). In the presence of either **Bet** or **Cha**, virtually no change is observed, consistent with no indicator displacement; but **Cho** and **BuCho** incubation (Figure 6c, blue /pink) cause a lower fluorescence peak, consistent with the "turn-off" images in Figure 5. The fluorescence was reduced further with a higher concentration of **Cho** (Figure S-26 and Table S-3). **DTMI** results in higher fluorescence than **DSMI** in cells (Figure 6c), which is reduced upon incubation with **TCC** host (see Figure S-27 and Table S-5). This "off" state is unaffected by **Bet** and **Cha** as before, but when **Cho** or **BuCho** are added to the incubation, the fluorescence is regenerated, although does not go back to the intensity level of **TCC•DTMI** (Figure 6c). All of this data matches the various confocal image results, and quantitates the effectiveness of the selective IDA process with **TCC** cavitand.

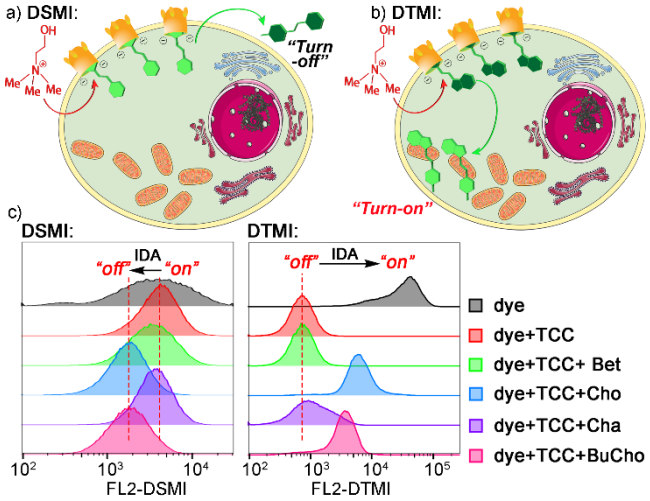

Figure 6. Flow cytometry. Representations of the a) "turn-on" and b) "turn-off" IDA processes. c) Flow cytometry histograms of live HeLa cells treated with dye, dye+host (pre-mix), and dye+host+substrate. [**dye**] = 5 μM, [**TCC**] = 5 μM (with **DSMI**) or 20 μM (with **DTMI**), [substrate] = 50 mM. Note: with **DTMI**, the substrate was added at the same time as the host•dye complex, for **DSMI**, the substrate or PBS was added afterwards. See Tables S-2 and S-4 for more information.

The **AMD•dye** complex in the HeLa cells is also fully capable of performing selective recognition and IDA sensing of the R-NMe_3^+ substrates, although the reporter output is different to that shown by **TCC**. Upon treatment of cells with **AMD•DTMI** and **Cho** or **BuCho** (see Figure 7a-c, S-21 and S-22), the **DTMI** dye is expunged from the cavitand, relocates to its preferred nucleotide-rich organelles, and a significant enhancement in emission is seen. The fluorescence increase is very strong – the images in Figure 7c and 7d were taken at a lower gain than those in Figure 7a/b (see Figure S-21 for images with identical gain) so that the location of the dye could be easily visualized; the original images are far too bright to see any details. The enhancement of **DTMI** fluorescence is less when bound in **AMD** than **TCC**,[17f] so the "turn-on" effect upon release from the host and incorporation in nucleotides is much larger. These fluorescence change trends were also observed in flow cytometry (Figure S-29 and Table S-7). These results support that **DTMI** can act as a turn-on sensor with **AMD,** as competitive binding of **Cho** removes the cavitand-based quenching. Similarly, **DSMI** can be quenched by **AMD**, and the fluorescence can be turned back on by incubation with **Cho**, as confirmed by both microscopy (Figure S-23 – S-24) and flow cytometry (Figure S-28 and Table S-6).

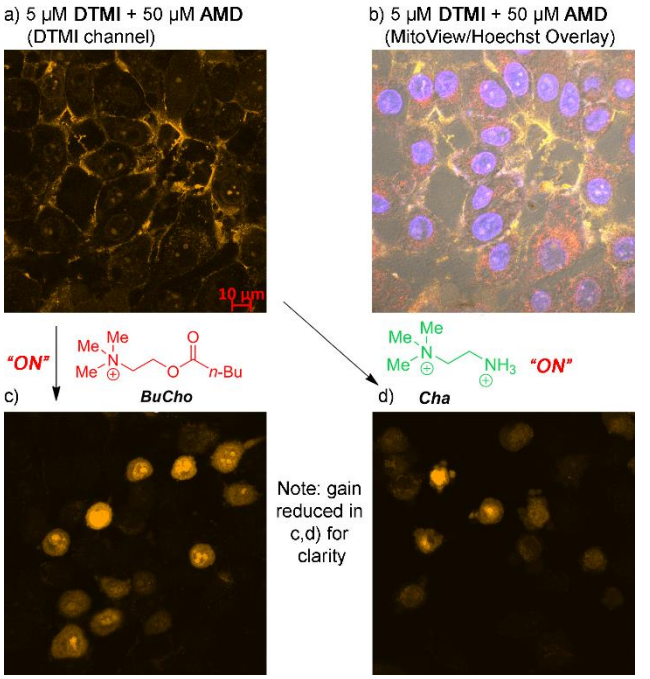

Figure 7. Sensing with AMD Host. Confocal fluorescence images of live HeLa cells treated by: a) & b) **AMD•DTMI** (pre-mix, 50 μM, 5 μM), c) **AMD•DTMI** (pre-mix, 50 μM, 5 μM) + 100 mM **BuCho**, and d) **AMD•DTMI** (pre-mix, 50 μM, 5 μM) + 100 mM **Cha** for 1 h, respectively. Images a) and b) were captured using the same samples at the same location, but a) shows only **DTMI** channel, b) is the Merged image of **DTMI**, Hoechst 33342, MitoView650, and Bright Field channels. All the default settings (see Supporting Information) were applied to the images a) and b). Images c) and d) were captured under a lower Gain of **DTMI** channel = 700.0.

The other notable difference is that **AMD** can detect cholamine (**Cha**), which was not observed with **TCC**. Betaine (**Bet**) causes no increase of dye fluorescence with any of the hosts, but as can be seen in Figure 7d, **DTMI** displacement is possible upon cholamine binding in **AMD**. The reasons for the greater ability of cholamine to displace the dye from **AMD** (as opposed to **TCC**) are not obvious: the binding affinity of different R-NMe_3^+ guests for differently charged hosts is highly variable, depending on conditions,[17b] and this illustrates that binding affinities in water do not necessarily translate to those in cellular media. Overall, the various cavitand/dye complexes are a powerful tool for selective target binding and sensing in cells: varying the dye allows different detection methodologies (either ("turn-on" or "turn-off"), whereas changing the nature of the cavitand allows differential selectivity for different R-NMe_3^+ substrates. Whereas **Cho**/**BuCho** are always strongly detected and **Bet** is never bound by cavitands, **Cha** detection can be tailored depending on

host structure. The combination of differently structured dyes and hosts enables tailored detection for different targets, even in challenging cellular environments.

CONCLUSIONS

Here, we have shown that multiple different water-soluble deep cavitands can perform selective cavity-based molecular recognition in cells, perform selective indicator-displacement-based sensing of choline derivatives and also control the intracellular location of bound targets. By varying the nature of the host and/or the dye used, different sensor outputs can be used for choline sensing, either "turn-on" or "turn-off". Binding selectivity is controlled by the host: strong guests such as choline and butyrylcholine can be easily detected, whereas less well-bound substrates such as betaine are ignored. The sensing is tolerant of all the competitive substrates present in the cell. The most striking property of the hosts is their ability to relocate substrates in the cell: the flat cationic styrylpyridinium dyes naturally gravitate towards nucleic acid-rich organelles, but the lipophilic cavitands mainly reside in the outer membrane. The cavitands are not "locked" in the membrane, but can traverse the cell to bind their targets and relocate them in membrane environments. This type of recognition is very rare with small molecule macrocycles: while common macrocyclic hosts have been shown to deliver cargo to cellular interiors, study of their cellular partitioning is often ignored. These observations add to the toolbox of applications shown by flexible, self-folding deep cavitands in biorecognition and sensing. It is also worth noting that incubation of the cells with these host:guest systems did not cause substantial cell death (Figures S-31 – S-33), and the components are not cytotoxic at the concentrations used.[19]

EXPERIMENTAL

General Information. Cavitands **TCC**,[18a] **AMD**,[17f] as well as fluorophores **DSMI**[17f] and **DTMI**[17f] were synthesized according to literature procedures. ^{1}H and ^{13}C spectra were recorded on Bruker Avance NEO 400 MHz or Bruker Avance 600 MHz NMR spectrometer. The spectrometers were automatically tuned and matched to the correct operating frequencies. Proton (^{1}H) and carbon (^{13}C) chemical shifts are reported in parts per million (δ) with respect to tetramethylsilane (TMS, δ=0), and referenced internally. Deuterated NMR solvents were obtained from Cambridge Isotope Laboratories, Inc., Andover, MA, and used without further purification. All other materials, including choline chloride, betaine, cholamine chloride and butyrylcholine chloride were purchased from Aldrich Chemical Company (St. Louis, MO), or Fisher Scientific (Fairlawn, NJ), and were used as received. Solvents were dried through a commercial solvent purification system (Pure Process Technologies, Inc.). Human cervical adenocarcinoma HeLa cell line was obtained from the American Type Culture Collection (ATCC). The cell culture medium was prepared by adding 50 mL Fetal Bovine Serum (FBS) and 6 mL Penicillin Streptomycin 100X Solution into 500 mL Dulbecco's Modified Eagle Medium (DMEM)/High glucose with L-glutamine, sodium pyruvate. The cells were grown in sterile petri dishes 100 mm × 15 mm or tissue culture dishes 60 mm × 15 mm. 6-well clear multiwell plates were used to grow cell samples for flow cytometry. Glass bottom cell culture dishes 15mm were used in confocal microscopy experiments. The incubation condition was 37 °C with 5% CO_2 in humid Forma Series II Water-Jacketed CO_2 Incubator. Phosphate buffered saline (PBS) pH 7.4 (1×) was used for sample dilution and washing cells. 0.25% Trypsin, 0.1% EDTA in HBSS w/o calcium, magnesium and sodium bicarbonate was used to release adherent cells. Cell Counting Kit-8 was purchased from Fisher Scientific and Selleckchem.com. 96-well, cell culture-treated, flat-bottom microplate was used for cell culture in CCK-8 assay.

Cell counting: HeLa cells were detached using trypsin solution, then well dispersed in cell culture medium. 10 μL cell suspensions were mixed with 10 μL Trypan Blue 0.4%, 0.85% NaCl, then the mixture was pipetted into dual-chamber cell counting slide, which was inserted in TC20 Automated cell counter (Bio-Rad) to test the live cell concentration.

Cell treatment procedures:

1) *Pre-mix **Host•Dye**:* 1 mL sample solution containing the dye and cavitand pre-mixed in PBS was added into cell culture dish for 1 h incubation with cells. (e.g., **TCC•DSMI**). 1a) *Pre-mix **Host•Dye** then **Substrate**:* 1 mL sample solution containing the dye and cavitand pre-mixed in PBS was added to treat the cells for the first hour; then the **Host•Dye** complex was removed before washing twice with 1 mL PBS; substrate molecules dissolved in PBS was used for the second hour treatment. (e.g., pre-mix **TCC•DSMI** then **Cho**). 1b) *Pre-mix **Host•Dye** + **Substrate**:* 1 mL sample solution containing the dye, cavitand and substrate pre-mixed in PBS was added into cell culture dish for 1 h incubation with cells. (e.g., pre-mix **TCC•DSMI** + **Cho**)

2) *Seq-mix **Dye** then **Host**:* 1 mL sample solution of the dye diluted in PBS was added for 1 h cell treatment and removed before washing cells twice with 1 mL PBS; then 1 mL sample solution of the cavitand diluted in PBS was added for 0 – 90 min cell treatment. (e.g., seq-mix **DTMI** then **TCC**)

Confocal microscopy: HeLa cells were cultivated in a glass bottomed cell culture dish with 6×10^5 cells/well and incubated for 24 h in a humid, 5% CO_2 incubator at 37 °C. After removing the medium, cells were washed twice with 1 mL PBS. The cell treatments were conducted at 37 ^{0}C, 5% CO_2 according to the procedure above.

1) For all the conditions except *Seq-mix **DTMI** then **TCC***, the sample solution was removed following by washing cells twice with 1 mL PBS, then cells were incubated with 1 mL DMEM/High Glucose containing 2 μg/mL Hoechst 33342 and 100 nM MitoView650, at ambient temperature. Before imaging, cells were washed with 1 mL PBS twice. 1mL PBS was added in the dish for imaging. The images were captured under a Zeiss LSM 880 Elyra confocal microscope with AxioObserver, and objective alpha Plan-Apochromat 100×/1.46 Oil DIC. 2) In the case of *Seq-mix **DTMI** then **TCC***, the **TCC** solution was retained in the confocal cell culture dish during imaging without adding Hoechst 33342 and MitoView650. The imaging was conducted with a Zeiss LSM 880 Elyra confocal microscope with AxioObserver, and objective alpha Plan-Apochromat 40×/1.4 Oil DIC M27. See Supporting Information for more setting information.

Flow cytometry: HeLa cells were cultivated in 6-well cell culture plates with 6×10^5 cells/well, incubated for 2 days in a humid, 5% CO_2 incubator at 37 °C. The cell treatments were conducted at 37 ^{0}C, 5% CO_2 according to the procedure above. After incubation, solution was aspirated, and cells were washed with 1 mL PBS twice and detached by trypsin solution for 3 min. 1 mL of cell culture medium

was added to quench trypsin, and cells were centrifuged at 500G for 3 min, followed by two further washes with 1 mL PBS. Harvested cells were kept on ice. Cells were acquired using a BD FACSCanto II flow cytometer with **DSMI**/**DTMI** fluorescence detected: Ex 488 nm, Em 564–606 nm (PE channel), forward scatter detection: photodiode with 488/10 bandpass filter, side scatter detection: PMT with 488/10 bandpass filter. 100,000 cells were collected. An unstained control (cells treated by PBS) was used to determine **DSMI**/**DTMI** positivity. Analysis was performed using FlowJo 10.8.1. Cells were gated to exclude debris using the SSC-A vs. FSC-A. Live cells were then gated to exclude doublets (FSC-H vs. FSC-A). Subsets were observed by gating SSC-A versus **DSMI**/**DTMI**. Please see Figure S-30 for gating strategy.

ASSOCIATED CONTENT

Supporting Information

All confocal microscopy images, flow cytometry and cytotoxicity data. This material is available free of charge via the Internet at http://pubs.acs.org.

AUTHOR INFORMATION

Corresponding Authors

* E-mail: richard.hooley@ucr.edu; wenwan.zhong@ucr.edu

ACKNOWLEDGMENTS

The authors would like to thank the National Science Foundation (CHE-1707347 to R. J. H. and W. Z.) and the National Institutes of Health (R01DA048815 to E. H. W.) for support, Prof. Joseph Genereux for the use of a cell counter, and Prof. Yinsheng Wang for a generous donation of HeLa cells.

REFERENCES

(1) (a) Pinalli, R.; Pedrini, A.; Dalcanale, E. Biochemical sensing with macrocyclic receptors. *Chem. Soc. Rev.* **2018**, *47*, 7006–7026. (b) van Dun, S.; Ottmann, C.; Milroy, L.-G.; Brunsveld, L. Supramolecular chemistry targeting proteins. *J. Am. Chem. Soc.* **2017**, *139*, 13960–13968.

(2) (a) Deng, C.-L.; Murkli, S. L.; Isaacs, L. D. Supramolecular hosts as in vivo sequestration agents for pharmaceuticals and toxins. *Chem. Soc. Rev.* **2020**, *49*, 7516–7532. (b) Crini, G. Review: a history of cyclodextrins. *Chem. Rev.* **2014**, *114*, 10940–10975. (c) Assaf, K. I.; Nau, W. M. Cucurbiturils: from synthesis to high-affinity binding and catalysis. *Chem. Soc. Rev.* **2015**, *44*, 394–418. (d) Beaver, J. E.; Waters, M. L. Molecular recognition of Lys and Arg methylation. *ACS Chem. Biol.* **2016**, *11*, 643–653. (e) Guo, D.-S.; Uzunova, V. D.; Su, X.; Liu, Y.; Nau, W. M. Operational calixarene-based fluorescent sensing systems for choline and acetylcholine and their application to enzymatic reactions. *Chem. Sci.* **2011**, *2*, 1722–1734. (f) Ogoshi, T.; Yamagishi, T.-a.; Nakamoto, Y. Pillar-shaped macrocyclic hosts pillar[n]arenes: new key players for supramolecular chemistry. *Chem. Rev.* **2016**, *116*, 7937–8002. (g) Hooley, R. J.; Rebek, J. Chemistry and catalysis in functional cavitands. *Chem. Biol.* **2009**, *16*, 255–264.

(3) (a) Beatty, M. A.; Hof, F. Host–guest binding in water, salty water, and biofluids: general lessons for synthetic, bio-targeted molecular recognition. *Chem. Soc. Rev.* **2021**, *50*, 4812–4832. (b) Krämer, J.; Kang, R.; Grimm, L. M.; De Cola, L.; Picchetti, P.; Biedermann, F. Molecular probes, chemosensors, and nanosensors for optical detection of biorelevant molecules and ions in aqueous media and biofluids. *Chem. Rev.* **2022**, *122*, 3459–3636. (c) Beatty, M. A.; Selinger, A. J.; Li, Y.; Hof, F. Parallel synthesis and screening of supramolecular chemosensors that achieve fluorescent turn-on detection of drugs in saliva. *J. Am. Chem. Soc.* **2019**, *141*, 16763–16771. (d) Hu, C.; Grimm, L.; Prabodh, A.; Baksi, A.; Siennicka, A.; Levkin, P. A.; Kappes, M. M.; Biedermann, F. Covalent cucurbit[7]uril–dye conjugates for sensing in aqueous saline media and biofluids. *Chem. Sci.* **2020**, *11*, 11142–11153. (e) Hu, C.; Jochmann, T.; Chakraborty, P.; Neumaier, M.; Levkin, P. A.; Kappes, M. M.; Biedermann, F. Further dimensions for sensing in biofluids: distinguishing bioorganic analytes by the salt-induced adaptation of a cucurbit [7] uril-based chemosensor. *J. Am. Chem. Soc.* **2022**, *144*, 13084–13095. (f) Harrison, E. E.; Waters, M. L. Application of an imprint-and-report sensor array for detection of the dietary metabolite trimethylamine N-oxide and its precursors in complex mixtures. *Angew. Chem. Int. Ed.* **2022**, *61*, e202205193. (g) Liu, Y.; Minami, T.; Nishiyabu, R.; Wang, Z.; Anzenbacher, P., Jr. Sensing of carboxylate drugs in urine by a supramolecular sensor array. *J. Am. Chem. Soc.* **2013**, *135*, 7705–7712. (h) Schramm, M. P.; Hooley, R. J.; Rebek, J. Guest recognition with micelle-bound cavitands. *J. Am. Chem. Soc.* **2007**, *129*, 9773–9779.

(4) Jordan, J. H.; Ashbaugh, H. S.; Mague, J. T.; Gibb, B. C. Buffer and salt effects in aqueous host–guest systems: screening, competitive binding, or both? *J. Am. Chem. Soc.* **2021**, *143*, 18605–18616.

(5) Thomas, S. S.; Tang, H.; Bohne, C. Non-innocent Role of Na^+ ions in the binding of the n-phenyl-2-naphthylammonium cation as a ditopic guest with cucurbit[7]uril. *J. Am. Chem. Soc.* **2019**, *141*, 9645–9654.

(6) Pan, Y.-C.; Hu, X.-Y.; Guo, D.-S. Biomedical applications of calixarenes: state of the art and perspectives. *Angew. Chem. Int. Ed.* **2021**, *60*, 2768–2794.

(7) (a) Sedgwick, A. C.; Brewster, J. T.; Wu, T.; Feng, X.; Bull, S. D.; Qian, X.; Sessler, J. L.; James, T. D.; Anslyn, E. V.; Sun, X. Indicator displacement assays (IDAs): the past, present and future. *Chem. Soc. Rev.* **2021**, *50*, 9–38. (b) You, L.; Zha, D.; Anslyn, E. V. Recent advances in supramolecular analytical chemistry using optical sensing. *Chem. Rev.* **2015**, *115*, 7840–7892.

(8) (a) Jiang, S.; Yang, J.; Ling, L.; Wang, S.; Ma, D. Supramolecular fluorescent probes for the detection of reactive oxygen species discovered via high-throughput screening. *Anal. Chem.* **2022**, *94*, 5634–5641. (b) Jia, J.; Wen, H.; Zhao, S.; Wang, L.; Qiao, H.; Shen, H.; Yu, Z.; Di, B.; Xu, L.; Hu, C. Displacement induced off–on fluorescent biosensor targeting IDO1 activity in live cells. *Anal. Chem.* **2019**, *91*, 14943–14950.

(9) Chinai, J. M.; Taylor, A. B.; Ryno, L. M.; Hargreaves, N. D.; Morris, C. A.; Hart, P. J.; Urbach, A. R. Molecular recognition of insulin by a synthetic receptor. *J. Am. Chem. Soc.* **2011**, *133*, 8810–8813.

(10) (a) Samanta, S. K.; Moncelet, D.; Briken, V.; Isaacs, L. Metal–organic polyhedron capped with cucurbit[8]uril delivers doxorubicin to cancer cells. *J. Am. Chem. Soc.* **2016**, *138*, 14488–14496. (b) Ganapati, S.; Grabitz, S. D.; Murkli, S.; Scheffenbichler, F.; Rudolph, M. I.; Zavalij, P. Y.; Eikermann, M.; Isaacs, L. Molecular containers bind drugs of abuse in vitro and reverse the hyperlocomotive effect of methamphetamine in rats. *ChemBioChem* **2017**, *18*, 1583–1588.

(11) Sasmal, R.; Das Saha, N.; Schueder, F.; Joshi, D.; Sheeba, V.; Jungmann, R.; Agasti, S. S. Dynamic host–guest interaction enables autonomous single molecule blinking and super-resolution imaging. *Chem. Commun.* **2019**, *55*, 14430–14433.

(12) (a) Geng, W.-C.; Ye, Z.; Zheng, Z.; Gao, J.; Li, J.-J.; Shah, M. R.; Xiao, L.; Guo, D.-S. Supramolecular bioimaging through signal amplification by combining indicator displacement assay with Förster resonance energy transfer. *Angew. Chem. Int. Ed.* **2021**, *60*, 19614–19619. (b) Tian, H.-W.; Chang, Y.-X.; Hu, X.-Y.; Shah, M. R.; Li, H.-B.; Guo, D.-S. Supramolecular imaging of spermine in cancer cells. *Nanoscale* **2021**, *13*, 15362–15368. (c) Gao, J.; Li, J.; Geng, W.-C.; Chen, F.-Y.; Duan, X.; Zheng, Z.; Ding, D.; Guo, D.-S. Biomarker displacement activation: a general host–guest strategy for targeted phototheranostics in vivo. *J. Am. Chem. Soc.* **2018**, *140*, 4945–4953.

(13) Norouzy, A.; Azizi, Z.; Nau, W. M. Indicator displacement assays inside live cells. *Angew. Chem. Int. Ed.* **2015**, *54*, 792–795.

(14) Tommasone, S.; Talotta, C.; Gaeta, C.; Margarucci, L.; Monti, M. C.; Casapullo, A.; Macchi, B.; Prete, S. P.; Ladeira De Araujo, A.; Neri, P. Biomolecular fishing for calixarene partners by a chemoproteomic approach. *Angew. Chem. Int. Ed.* **2015**, *54*, 15405–15409.

(15) Geng, W.-C.; Jia, S.; Zheng, Z.; Li, Z.; Ding, D.; Guo, D.-S. A Noncovalent fluorescence turn-on strategy for hypoxia imaging. *Angew. Chem. Int. Ed.* **2019**, *58*, 2377–2381.

(16) Zhong, W.; Hooley, R. J. Combining excellent selectivity with broad target scope: biosensing with arrayed deep cavitand hosts. *Acc. Chem. Res.* **2022**, *55*, 1035–1046.

(17) (a) Liu, Y.; Perez, L.; Mettry, M.; Easley, C. J.; Hooley, R. J.; Zhong, W. Self-aggregating deep cavitand acts as a fluorescence displacement sensor for lysine methylation. *J. Am. Chem. Soc.* **2016**, *138*, 10746–10749. (b) Liu, Y.; Perez, L.; Mettry, M.; Gill, A. D.; Byers, S. R.; Easley, C. J.; Bardeen, C. J.; Zhong, W.; Hooley, R. J. Site selective reading of epigenetic markers by a dual-mode synthetic receptor array. *Chem. Sci.* **2017**, *8*, 3960–3970. (c) Liu, Y.; Lee, J.; Perez, L.; Gill, A. D.; Hooley, R. J.; Zhong, W. Selective sensing of phosphorylated peptides and monitoring kinase and phosphatase activity with a supramolecular tandem assay. *J. Am. Chem. Soc.* **2018**, *140*, 13869–13877. (d) Chen, J.; Hickey, B. L.; Wang, L.; Lee, J.; Gill, A. D.; Favero, A.; Pinalli, R.; Dalcanale, E.; Hooley, R. J.; Zhong, W. Selective discrimination and classification of G-quadruplex structures with a host–guest sensing array. *Nat. Chem.* **2021**, *13*, 488–495. (e) Chen, J.; Gill, A. D.; Hickey, B. L.; Gao, Z.; Cui, X.; Hooley, R. J.; Zhong, W. Machine learning aids classification and discrimination of noncanonical DNA folding motifs by an arrayed host:guest sensing system. *J. Am. Chem. Soc.* **2021**, *143*, 12791–12799. (f) Chen, J.; Hickey, B. L.; Gao, Z.; Raz, A. A. P.; Hooley, R. J.; Zhong, W. Sensing base modifications in non-canonically folded DNA with an optimized host:guest sensing array. *ACS Sens.* **2022**, *7*, 2164–2169. (g) Gill, A. D.; Hickey, B. L.; Zhong, W.; Hooley, R. J. Selective sensing of THC and related metabolites in biofluids by host:guest arrays. *Chem. Commun.* **2020**, *56*, 4352–4355. (h) Hickey, B. L.; Chen, J.; Zou, Y.; Gill, A. D.; Zhong, W.; Millar, J. G.; Hooley, R. J. Enantioselective sensing of insect pheromones in water. *Chem. Commun.* **2021**, *57*, 13341–13344.

(18) (a) Biros, S. M.; Ullrich, E. C.; Hof, F.; Trembleau, L.; Rebek, J. Kinetically stable complexes in water: the role of hydration and hydrophobicity. *J. Am. Chem. Soc.* **2004**, *126*, 2870–2876. (b) Hooley, R.J.; Van Anda, H. J.; Rebek, J., Jr. Extraction of hydrophobic species into a water-soluble synthetic receptor *J. Am. Chem. Soc.*, **2007**, *129*, 13464–13473.

(19) Ghang, Y.-J.; Schramm, M. P.; Zhang, F.; Acey, R. A.; David, C. N.; Wilson, E. H.; Wang, Y.; Cheng, Q.; Hooley, R. J. Selective cavitand-mediated endocytosis of targeted imaging agents into live cells. *J. Am. Chem. Soc.* **2013**, *135*, 7090–7093.

(20) Li, H.; Li, Y.; Zhang, H.; Xu, G.; Zhang, Y.; Liu, X.; Zhou, H.; Yang, X.; Zhang, X.; Tian, Y. Water-soluble small-molecule probes for RNA based on a two-photon fluorescence "off–on" process: systematic analysis in live cell imaging and understanding of structure–activity relationships. *Chem. Commun.* **2017**, *53*, 13245–13248.

(21) (a) Liu, Y.; Liao, P.; Cheng, Q.; Hooley, R. J. Protein and small molecule recognition properties of deep cavitands in a supported lipid membrane determined by calcination-enhanced SPR spectroscopy. *J. Am. Chem. Soc.* **2010**, *132*, 10383–10390. (b) Perez, L.; Caulkins, B. G.; Mettry, M.; Mueller, L. J.; Hooley, R. J. Lipid bilayer environments control exchange kinetics of deep cavitand hosts and enhance disfavored guest conformations. *Chem. Sci.* **2018**, *9*, 1836–1845.

TOC Graphic: